SYMPOSIUM

Shifts in Mutation Bias Promote Mutators by Altering the Distribution of Fitness Effects*

Marwa Z. Tuffaha,[1] Saranya Varakunan,[1] David Castellano,[2] Ryan N. Gutenkunst,[2] and Lindi M. Wahl[1,†]

1. Western University, London, Ontario N6A 5B7, Canada; 2. Department of Molecular and Cellular Biology, University of Arizona, Tucson, Arizona 85721

Submitted September 29, 2022; Accepted March 15, 2023; Electronically published August 23, 2023

Online enhancements: supplemental PDF.

ABSTRACT: Recent experimental evidence demonstrates that shifts in mutational biases—for example, increases in transversion frequency—can change the distribution of fitness effects of mutations (DFE). In particular, reducing or reversing a prevailing bias can increase the probability that a de novo mutation is beneficial. It has also been shown that mutator bacteria are more likely to emerge if the beneficial mutations they generate have a larger effect size than observed in the wild type. Here, we connect these two results, demonstrating that mutator strains that reduce or reverse a prevailing bias have a positively shifted DFE, which in turn can dramatically increase their emergence probability. Since changes in mutation rate and bias are often coupled through the gain and loss of DNA repair enzymes, our results predict that the invasion of mutator strains will be facilitated by shifts in mutation bias that offer improved access to previously undersampled beneficial mutations.

Keywords: mutation bias, mutation spectra, mutation rate, mutator, bacteria, microbial evolution.

Introduction

De novo mutation is foundational to both genetic diversity and adaptive innovation; mutation rates vary both among taxa (Lynch et al. 2016) and across the genome (Hodgkinson and Eyre-Walker 2011; Martincorena and Luscombe 2013; Monroe et al. 2022) and can respond rapidly to selective pressure (Wei et al. 2022).

Mutations, however, occur in many forms; single-nucleotide substitutions are frequently classified as transitions, transversions, specific base-to-base substitutions, or substitutions in *n*-mer contexts, while insertions, deletions, or larger genome rearrangements likewise generate substantial genetic variation (Hodgkinson and Eyre-Walker 2011). Mutation-accumulation studies have allowed for detailed analyses of the rates and contexts of specific types of mutations, the "mutation spectrum" (Katju and Bergthorsson 2019).

These data have brought to light the fact that the mutation spectrum is biased—in other words, certain classes of mutations occur more frequently than others (Foster et al. 2015; Katju and Bergthorsson 2019). For example, the frequency of transitions can range from less than 5% to more than 95% in bacterial strains that express different DNA repair genes (Lee et al. 2012; Foster et al. 2015), and substantial changes in the mutation spectrum have also been detected in human populations (Harris and Pritchard 2017). A wealth of recent work has demonstrated that this underlying mutation bias influences and is ultimately echoed in the spectrum of adaptive substitutions (Stoltzfus and Yampolsky 2009; Stoltzfus and McCandlish 2017; Soares et al. 2021), even at high mutation rates (Gomez et al. 2020), as demonstrated for fitness landscapes in transcription factor binding sites (Cano and Payne 2020), for antibiotic resistance (Payne et al. 2019), for convergent mutations in protein sequences (Storz et al. 2019), and for thousands of amino acid changes observed in natural and experimental microbial populations (Cano et al. 2022). As formally derived elsewhere in this special section (Gitschlag et al. 2023), in the strong-selection/weak-mutation regime fixed substitutions are predicted to be enriched for mutations that occur at high rates. Taken together, this body of work demonstrates that in multiple evolutionary contexts, the spectrum of likely mutations is strongly reflected in the spectrum of adaptive substitutions.

* This article was presented as part of the 2022 Vice Presidential Symposium at the annual meetings of the American Society of Naturalists in Cleveland, Ohio.

† Corresponding author; email: lwahl@uwo.ca.

ORCIDs: Tuffaha, https://orcid.org/0000-0002-6285-0938; Wahl, https://orcid.org/0000-0003-1163-0940; Varakunan, https://orcid.org/0009-0004-0982-9410; Castellano, https://orcid.org/0000-0001-8778-6007; Gutenkunst https://orcid.org/0000-0002-8659-0579.

  https://doi.org/10.1086/726010

What are the implications of this result? Taking transitions and transversions as an example, the result above implies that beneficial transitions will be more likely to occur and fix, during adaptation, in a population with transition-biased mutations. If there is no a priori reason to expect that beneficial mutations are more likely to be transitions or transversions (Stoltzfus and Norris 2015), this implies that beneficial transversions will be comparatively undersampled as adaptation proceeds. Thus, after a period of adaptation with a transition bias, reducing the bias to sample more transversions—or even reversing it to oversample transversions—can offer access to previously unsampled beneficial mutations. This effect has been recently demonstrated in bacteria, in which shifts in the mutation bias increased the fraction of new mutations that were beneficial (Sane et al. 2023). Simulations of adaptive walks likewise demonstrated a robust effect in which, after a period of adaptation, any reduction or reversal in the existing mutation bias altered the distribution of fitness effects of mutations (DFE), increasing the fraction of beneficial mutations (Sane et al. 2023). This idea, that changing the mutation spectrum could alter (MacLean et al. 2010) or in fact increase the beneficial fraction of the DFE, has been previously suggested (Maharjan and Ferenci 2017), and changes in the DFE have been demonstrated for bacterial mutators evolving antibiotic resistance (Couce et al. 2013).

Mutators (microbial strains that increase the mutation rate by one or several orders of magnitude) are frequently observed in experimental (Treffers et al. 1954; Miyake 1960; Sniegowski et al. 1997; Shaver et al. 2002; Wielgoss et al. 2012; Wei et al. 2022), natural (LeClerc et al. 1996; Matic et al. 1997; Oliver et al. 2000; Giraud et al. 2001; Richardson et al. 2002; Jiang et al. 2021), and clinical (Couce et al. 2016; Raghavan et al. 2019; Ridderberg et al. 2020) populations; the mutator phenotype is also prevalent in human tumors, which likewise reproduce asexually (Fox et al. 2013). This phenomenon is understood to occur in asexual evolution because a mutation that increases the mutation rate (typically the loss of function of a mismatch repair enzyme; Denamur and Matic 2006) hitchhikes with the de novo beneficial mutation produced in the mutator strain (Maynard Smith and Haigh 1974; Sniegowski et al. 1997). The dynamics of mutation rate modifiers have been well studied both analytically and in simulation; mutators are disfavored in the presence of genetic exchange (Johnson 1999; Tenaillon et al. 2000) but favored in fluctuating environments (Leigh 1970; Travis and Travis 2002) or when multiple mutations are required for adaptation either simultaneously (Taddei et al. 1997; Tenaillon et al. 1999) or in sequence (Tanaka et al. 2003). On smooth fitness landscapes, the complex interplay among genetic drift, deleterious load, and competition between wild-type and mutator strains is well understood analytically (Kessler and Levine 1998; Wylie et al. 2009).

Couce et al. (2013) studied two mutator strains of *Escherichia coli*, each of which increased specific classes of transversions. These changes in mutation spectrum resulted in changes to the DFE for both strains relative to the wild type. To investigate whether these changes in spectrum could influence mutator emergence, populations were simulated in which the fraction of beneficial mutations was held constant, and every beneficial mutation had fixed effect size s in the wild type and effect size σs in mutators. Results predicted that if the effect size of the beneficial mutation in a mutator strain was increased relative to the wild type, even by a modest amount, the emergence of mutator strains was substantially increased (Couce et al. 2013).

Here, we use theory and simulations to explicitly investigate how a shift in bias affects the DFE, changing both the fraction of mutations that are beneficial and the mean selective effect of beneficial mutations. Using full population simulations, we demonstrate robust benefits of reducing or reversing the mutation bias after a period of adaptation. We investigate the fate of mutations that change the bias, change the mutation rate, or change both the bias and the mutation rate. We demonstrate that mutations that reduce or reverse the bias and increase the mutation rate are most likely to emerge and that this effect is nonlinear; a bias shift can dramatically improve the chances of mutator fixation, through the resulting changes in the DFE. Since many loss-of-function mutations affect both mutation rate and bias, our results suggest that shifts in mutation bias may powerfully facilitate the invasion of mutator strains.

Theory

The Distribution of Fitness Effects

Suppose an individual with fitness W has an offspring that carries a mutation. If the offspring has fitness W', the fitness effect of the mutation is defined as $s = W'/W - 1$, where s can be negative, zero, or positive. The DFE can then be defined as the distribution of such values of s from all possible mutations for a single ancestor genome. This definition, however, assumes that the organism has equal access to all mutations, whereas in reality certain classes of mutations are typically over- or underrepresented. It is therefore important to draw the distinction between the DFE of all possible mutations, $\mathrm{DFE}_{\mathrm{all}}$, which is often of theoretical interest, and the mutation-weighted (i.e., bias-weighted) DFE, DFE_{β}. The latter is computed by weighting each entry in $\mathrm{DFE}_{\mathrm{all}}$ by the rate at which it is expected to occur. We emphasize that DFE_{β} is the DFE that is accessible experimentally through mutation-accumulation experiments and, critically, accessed by the organism during evolution. In the sections to follow, we will use f to denote the fraction of mutations in a DFE that are beneficial, adding subscripts

to denote particular cases, such as f_{all} or f_β. For a list of symbols and their definitions, see table 1.

A second definition that requires clarification is the concept of unbiased mutation. In each individual, a particular locus (or site) in the genome exists in a particular state (e.g., as a particular nucleotide, but the argument extends to amino acids or more general "alleles"). A number of other alternate states are possible at that locus. The mutation process is unbiased if each of these alternate states is accessed by mutation with equal probability. Thus, unbiased mutation does not depend on the underlying biochemistry of mutation or neutrality of effect; it depends only on the possible alternative states. As an example, a transition fraction of one-third is unbiased, because for any nucleotide, one-third of the alternate states are reached via transitions. We define mutation classes as over- or undersampled relative to this unbiased expectation. (We also note that for some classes of mutations, such as GC → AT vs. AT → GC, the unbiased genome-wide mutation rate will depend on genome content; we will not treat these cases here.)

Table 1: Symbols used in the theoretical analysis

Symbol	Definition
M	Number of possible mutations
B	Number of possible beneficial mutations
n	Number of fixed mutations after a period of adaptive evolution
α	Fraction of mutations of type 1
β	Probability that a mutation that occurs is of type 1 (i.e., bias)
DFE_{all}	Distribution of fitness effects of all possible mutations
DFE_β	Bias-weighted distribution of fitness effects
f_{all}	Fraction of mutations that are beneficial ("beneficial fraction") in DFE_{all}
f_β	Beneficial fraction in DFE_β
f_i	Fraction of mutations of type i that are beneficial ($i \in \{1, 2\}$)
f_a	Beneficial fraction in the ancestor
μ	Mutation rate per genome per generation
F	Mutation rate multiplier in mutator strain
p_μ	Fraction of population with higher mutation rate
p_{bs}	Fraction of population with bias shift
$p_{\mu,bs}$	Fraction of population with higher mutation rate and bias shift
f_{wt}	Beneficial fraction in the wild type
f_{bs}	Beneficial fraction in the bias-shifted strain
G	Increase in beneficial fraction due to the bias shift
π_{wt}	Fixation probability of a beneficial mutation in the wild type
π_{bs}	Fixation probability of a beneficial mutation in the bias-shifted strain
H	Increase in fixation probability of a beneficial mutation due to the bias shift
d	Deleterious fraction in DFE_β
s_b	Selective advantage of new beneficial mutation
δ	Expected increase in beneficial effect due to a bias shift
ε	Expected reduction in deleterious effect due to a bias shift

This definition of unbiased mutation also allows us to define bias reinforcements, reductions, and reversals for cases when the mutation bias changes over time. A shift from transition-biased mutation to transversion-biased mutation is a bias reversal. A shift from transition-biased mutation to more extreme transition-biased mutation is a reinforcement. A shift from transition-biased mutation to a less extreme but still transition-biased mutation process is a bias reduction.

In the introduction, we provided a verbal argument that a reduction or reversal in an existing (historically prevailing) mutation bias increases the beneficial fraction of the DFE_β. Although the logic is straightforward, in the remainder of this section we demonstrate this effect mathematically, which allows us to carefully define the conditions and assumptions under which this expectation holds.

Consider an evolving population in which each individual has M possible mutations in two distinct classes (e.g., transitions and transversions). (The approach below can be generalized to any number of mutation classes, but we use two for clarity.) Let α be the fraction of possible mutations of type 1, such that there are αM mutations in the first class and $(1 - \alpha)M$ in the second. In the case of transitions as class 1 and transversions as class 2, the value of α is one-third.

Consider a particular "ancestor" genotype. Let B denote the total number of beneficial mutations out of the M possible mutations for the ancestor. Thus, the fraction of beneficial mutations in the ancestor, defined as f_a, is given by B/M. Now suppose that we have no a priori reason to assume that mutations of one type or another are more likely to be beneficial, nor do they have different beneficial effect sizes. Under the assumption that the beneficial DFEs are the same in the two classes of mutations, we expect αB potential beneficial mutations in the first class and $(1 - \alpha)B$ in the second, as shown in the first two rows of table 2.

Now assume that after a period of adaptive evolution, n beneficial mutations have fixed. For clarity, we will assume that mutations fix sequentially without competition (i.e., the strong-selection/weak-mutation regime), but this will be relaxed in the simulations to follow. If there is no mutation bias, beneficial mutations in each class will be equally likely to be sampled and reach fixation, so we expect αn fixations in the first mutation class and $(1 - \alpha)n$ in

Table 2: Values for numbers of mutations and beneficial fractions in the ancestor and in an evolved strain after n fixation events

	Total	Class 1 (e.g., Ti)	Class 2 (e.g., Tv)
Number of mutations:			
All possible	M	αM	$(1-\alpha)M$
Beneficial, available to ancestor	B	αB	$(1-\alpha)B$
Beneficial, fixed in evolved	n	βn	$(1-\beta)n$
Beneficial fractions:			
Ancestral (f_a)	$f_a = \frac{B}{M}$	$\frac{\alpha B}{\alpha M} = f_a$	$\frac{(1-\alpha)B}{(1-\alpha)M} = f_a$
Evolved, after n fixations	$\frac{B-n}{M} = f_a - \frac{n}{M}$	$\frac{\alpha B - \beta n}{\alpha M} = f_a - \left(\frac{\beta}{\alpha}\right)\frac{n}{M}$	$f_a - \frac{(1-\beta)}{(1-\alpha)}\frac{n}{M}$

Note: See text for details. Ti = transition; Tv = transversion.

the second. In contrast, suppose mutation bias has led to a different sampling ratio of mutations. While α is the fraction of all possible mutations that are in the first class, let β be the fraction of mutations that occur that are in the first class. We would then expect βn fixations in the first class and $(1-\beta)n$ in the second.

Without loss of generality, assume $\alpha < \beta$, such that class 1 is the oversampled class. As a realistic example, we consider a transition-biased organism, such that $\beta > 1/3$ of fixed mutations are transitions. This implies that mutation bias has led to the fixation of more beneficial mutations of type 1 and fewer of type 2 than expected under the theoretically defined unbiased mutation process (for recent empirical examples, see Cano et al. 2022).

At this point we must impose further assumptions regarding the fitness landscape. In reality, due to epistasis, each beneficial substitution may change the remaining number of beneficial mutations, both in its own class and in others. Even in the absence of epistasis, a given nucleotide could have two possible beneficial mutations; for example, both possible transversions could be beneficial, and after one transversion has fixed, the remaining transversion (now a transition) may or may not provide a further benefit. These complexities are captured in the simulation studies that follow. For analytical tractability, however, we will assume a smooth fitness landscape and that beneficial mutations are rare. In particular, each locus has at most a single beneficial mutation available.

In this simplified fitness landscape, it is straightforward to compute the fraction of remaining mutations in each class that are beneficial, f_1 and f_2, by simply subtracting the number of beneficial substitutions that have occurred. As shown in the last row of table 2, we find

$$f_1 = \frac{\alpha B - \beta n}{\alpha M} = f_a - \frac{\beta}{\alpha}\left(\frac{n}{M}\right). \quad (1)$$

Similarly,

$$f_2 = f_a - \frac{1-\beta}{1-\alpha}\left(\frac{n}{M}\right). \quad (2)$$

Since $\alpha < \beta$, it is clear that $f_1 < f_2$; the beneficial fraction for mutations in the oversampled class is less than the beneficial fraction in the undersampled class.

We can also compare the two DFEs defined above: (1) DFE_{all}, the DFE of all possible mutations that assumes equal access to all mutations, and (2) DFE_{β}, the mutation-weighted DFE that takes the bias into account. Let f_{all} and f_{β} denote the fractions of beneficial mutations in DFE_{all} and DFE_{β}, respectively, after this period of evolution. Since DFE_{all} samples class 1 mutations with probability α and class 2 with probability $(1-\alpha)$, we find

$$f_{\text{all}} = \alpha f_1 + (1-\alpha) f_2, \quad (3)$$

while similarly

$$f_{\beta} = \beta f_1 + (1-\beta) f_2. \quad (4)$$

Again, since $\alpha < \beta$ and $f_1 < f_2$, we find that $f_{\text{all}} > f_{\beta}$. Hence, the organism will access a smaller fraction of beneficial mutations than is potentially available.

This might change, however, if the mutation bias shifts. If the mutation bias shifts to β', then the bias-weighted DFE changes and the fraction of beneficial mutations becomes $f'_{\beta} = \beta' f_1 + (1-\beta') f_2$. There are two possibilities. First, the new bias reduces or reverses the previous bias. Taking as we did before the case when $\alpha < \beta$, a bias reduction occurs when $\alpha < \beta' < \beta$, while a reversal happens when β' is even lower than α. In either case (reduction or reversal), we find that $f'_{\beta} > f_{\beta}$; in other words, the new bias increases access to beneficial mutations. Second and in contrast, the new bias could reinforce the original bias, which occurs when $\beta' > \beta$. This yields $f'_{\beta} < f_{\beta}$ and thus

implies reduced access to beneficial mutations. Moreover, it is clear that these effects will be stronger when the difference $|\beta - \beta'|$ is bigger (i.e., when the reversal or the reinforcement has a greater magnitude).

In the simulations to follow, we illustrate examples of these effects where mutations are classified as transitions and transversions and in which we relax the assumptions of a smooth fitness landscape (no epistasis), of rare beneficial mutations, and of strong-selection/weak-mutation evolutionary dynamics.

Hitchhiking Probabilities

Some simple back-of-the-envelope calculations offer critical insights into the evolution of the mutation bias. We follow a heuristic argument described by Lenski (2004) and developed more formally by Wylie et al. (2009). Suppose a fraction p_μ of a population has an F-fold higher mutation rate but is otherwise identical to the wild type. The chance that the next beneficial mutation that sweeps through the population occurs in the mutator strain is then simply approximated by $p_\mu F$. Lenski gives a quantitative estimate of this factor for *Escherichia coli* mutators that segregate at an estimated frequency of 1×10^{-4} and have a 100-fold increase in mutation rate, predicting that about 1% of beneficial substitutions will occur in the mutator.

This argument naturally assumes that the DFE is identical in the wild type and mutator. In contrast, suppose a fraction p_{bs} of a population has a shift in mutation bias but has the same mutation rate as the wild type. If the bias shift reduces or reverses the wild-type bias, the bias-shifted strain will experience a G-fold higher beneficial fraction:

$$G = \frac{f_{\text{bs}}}{f_{\text{wt}}}, \tag{5}$$

where f_{wt} and f_{bs} denote the beneficial fraction of the DFE_β in the wild-type and bias-shifted strain, respectively. Assuming the effect size of beneficial mutations and the deleterious load are unchanged with the bias shift, the chance that the next beneficial mutation carries the bias-shifted strain to fixation is approximated by $p_{\text{bs}}G$.

If, in addition, the beneficial effect size is increased in the bias-shifted strain, then the expected fixation probability of a beneficial mutation in this strain, π_{bs}, will exceed the analogous expectation in the wild type, π_{wt}, such that beneficial mutations have an H-fold higher fixation probability if they occur in the bias-shifted background, where

$$H = \frac{\pi_{\text{bs}}}{\pi_{\text{wt}}}. \tag{6}$$

Overall, the fraction of beneficial fixations that occur in the bias-shifted strain is then $p_{\text{bs}}GH$.

A quantitative estimate of this factor is challenging. In bacteria, both environmental stress and the loss of function of specific DNA repair enzymes can cause bias shifts without a substantial change in mutation rate (Foster et al. 2015; Maharjan and Ferenci 2017; Shewaramani et al. 2017; Sane et al. 2023); however, it is difficult to estimate the frequency at which such mutations might segregate in natural populations. Nonetheless, in both experimental (Sane et al. 2023) and simulated fitness landscapes, as seen in the results to follow, both factors G and H (the relative advantage of bias-shifted strains) are modest, typically in the range of 1 to 2. In contrast, F, the mutation rate multiplier, can be a factor of 100 or more. We conclude that unless bias-shifted strains are maintained by the mutation-selection balance at frequencies that are several orders of magnitude higher than mutator strains, they will be much less likely than mutators to fix during adaptation.

However, suppose a fraction $p_{\mu,\text{bs}}$ of a population has both an increased mutation rate and a bias shift. This is in fact the most likely situation for loss-of-function mutations in DNA repair (Foster et al. 2015; Sane et al. 2023). The chance that a beneficial mutation carries this strain to fixation would then be $p_{\mu,\text{bs}}FGH$; in other words, the effects combine multiplicatively. We thus predict, in agreement with Couce et al. (2013), that bias shifts could powerfully affect the invasion rate of mutator strains.

The reasoning above neglects the effects of changes to the deleterious load when the bias or mutation rate is altered. Recall that for a mutation rate μ per genome and deleterious fraction d in DFE_β, the load is approximated by the product μd and is in fact independent of the deleterious effect size (Ewens 2012). Thus, a strain that increases the mutation rate only, by factor F, will experience an increased load of $F\mu d$. In contrast, for strains in which only a bias shift occurs, the deleterious fraction, d, will be reduced whenever the beneficial fraction, f, is increased (although this reduction is exactly concomitant only in very large populations in which the neutral fraction of the DFE is negligible). Thus, any bias shift that increases the beneficial fraction will reduce the load.

For a mutator strain in which both the mutation rate and bias are altered, both of these effects come into play. Depending on the relative magnitudes of the increase in mutation rate and reduction in the deleterious fraction, the mutator strain may carry a greater or lesser load than the wild type.

The magnitude of deleterious load will ultimately affect the fixation probability for beneficial mutations on the mutator background, reducing (and possibly reversing) the fixation advantage. For a mutator with an increased mutation rate $F\mu$, load overwhelms the expected selective

advantage of new beneficial mutations when $F\mu d > s_b$ or when the mutation rate multiple exceeds the critical value

$$F^*_\mu = \frac{s_b}{\mu d}. \quad (7)$$

In contrast, consider a bias shift that increases the expected beneficial effect by a factor $(1 + \delta)$ and also reduces the deleterious fraction by a factor $(1 - \epsilon)$. For a mutator in which both the bias and the mutation rate change, load overwhelms the selective advantage when $F\mu d(1 - \epsilon) > s_b(1 + \delta)$ or when F exceeds

$$F^*_{\mu,bs} = \frac{s_b(1 + \delta)}{\mu d(1 - \epsilon)}. \quad (8)$$

Since $F^*_{\mu,bs} > F^*_\mu$, these results predict that bias reductions and reversals not only will increase the invasion probability of mutator strains but will extend the range of mutation rates over which invasion is favored. Both of these predictions are verified in the simulation results to follow.

Simulation Methods

We simulated population evolution on the well-studied *NK* fitness landscape (Macken and Perelson 1989; Stoltzfus 2006). Each genotype is represented by a genomic sequence of length N, composed of four bases (A, C, G, T) such that mutations can be classified as transitions or transversions.

In an *NK* fitness landscape, the fitness of a sequence is simply calculated by adding the fitness contributions of all its loci. To incorporate epistasis, however, the fitness contribution of each locus depends not only on the state of the locus but on the states of K other randomly assigned loci. Thus, K determines the degree of epistasis (i.e., the number of loci epistatically coupled to each locus). For instance, for $K = 2$ and a given locus m, there are $4^{K+1} = 64$ different possible combinations for that locus and its two neighbors: AAA, AAC, AAG, ..., TTT. Every such combination is randomly assigned a uniformly distributed value from the interval (0, 1), which defines the fitness contribution of locus m.

Each individual in the population is assigned the following: (1) a genome sequence, which determines fitness; (2) a transition-to-transversion bias (Ti : Tv), where Ti = 1 − Tv gives the probability that a de novo mutation is a transition; and (3) a mutation rate μ per genome per generation. In some simulations the bias and/or mutation rate are fixed, while in other scenarios they are manipulated.

The population is initialized in generation 0 with a population size n_0, typically seeded with a number of random genotypes. Generations are discrete; the number of offspring for the ith genotype in generation j is Poisson distributed with mean

$$\lambda_{ij} = r_j\, n_{ij} \frac{w_{ij}}{\bar{w}_j}, \quad (9)$$

where n_{ij} and w_{ij} represent the number of individuals and the fitness of the ith genotype in generation j, respectively, while $\bar{w}_j$ is the mean fitness of the population in generation j. The variable $r_j = \exp(1 - (n_j/\kappa))$ is the Ricker factor in generation j, which limits overall population growth by comparing the total number of individuals in generation j, n_j, to the carrying capacity κ.

In every generation, mutations occur according to each genotype's mutation rate, μ_i. When a mutation occurs, it affects a randomly chosen nucleotide in the sequence, and the mutation is a transition or a transversion according to that genotype's bias. If the mutation is a transversion, one of the two possibilities (e.g., T → G or T → A) is chosen at random. Mutations occur during reproduction and when they occur, a single individual with the new genotype is added to the next generation, where the new individual inherits the parental mutation rate and bias.

We keep track of each distinct genotype in the population and number of individuals of that genotype, but we do not track the ancestry of every individual. Thus, to estimate—at a given generation—the divergence of the population from the initial population, we first identify the most common genotype in the population. We then compute the Hamming distance (number of nucleotide differences) between this genotype and each genotype in the founding population. We report the minimum of these Hamming distances as a measure of genetic divergence from the ancestral population. As a proxy for fixations, we also report the number of transitions and transversions by which the most common genotype differs from its closest match in the founding population. This is a proxy for two reasons: because true fixations may or may not occur in our genetically diverse full population simulations, and because two consecutive transversions at the same locus might lead to what would be counted as a transition.

In the results to follow, we perform invasion tests for mutant strains that change only the mutation bias but not the mutation rate, mutators that increase the mutation rate alone, and mutators that change both the rate and the bias, as illustrated in figure 1. Invasion tests are initiated in our simulations either by following the fate of an invading subpopulation at an initial frequency of 5% or by tracking the fate of a single randomly chosen individual. Because any single lineage has a high probability of becoming extinct even if it carries a selective advantage, the latter approach may require simulating a very large number of replicates. Thus, for computational efficiency, results in the

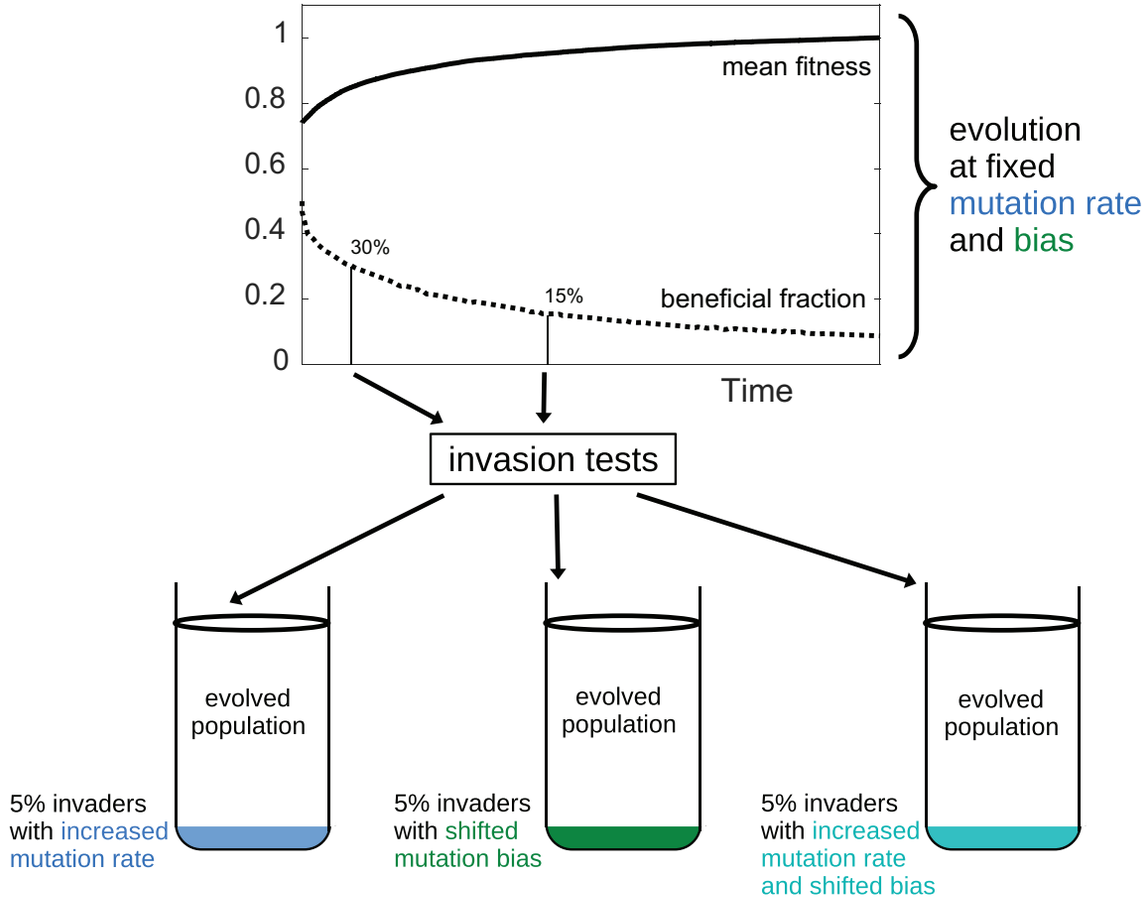

Figure 1: Schematic diagram of simulated invasion tests. For each replicate, we create a new fitness landscape, initiate a new population, and start evolution at time zero. Populations of initially random genotypes evolve with a fixed mutation rate and fixed transition-to-transversion bias. The mean population fitness (solid line) increases over time, while the fraction of mutations in the mutation-weighted distribution of fitness effects of mutations that are beneficial (dotted line) declines. When the mutation-weighted beneficial fraction, f_β, reaches 30%, we perform the three invasion tests illustrated. The same tests are repeated in new simulations but when the beneficial fraction in the evolving population reaches 15%.

main text were generated for an invading subpopulation. (Figure S1 shows results for the invasion of a single individual; we observed no qualitative differences in invasion results in the two cases.) We also note that predicted outcomes with an invader frequency of 5% are amenable to empirical testing.

Populations in these simulations, however, are genetically diverse; in some parameter regimes the average number of segregating strains is of order 100. The use of an invading subpopulation thus necessitates the choice of a genotype for the invading strain. Since the most common genotype in the population is typically also the fittest, using this genotype for the invading strain biases the results in favor of invasion. Instead, we initiate the mutant subpopulation by changing the mutation rate and/or bias in a random 5% of individuals in the population. Thus, the invading subpopulation has on average the same genetic diversity (and, critically, the same genetic load) as the ancestral population.

Similar to a competition experiment, we then track whether this subpopulation invades. We perform invasion tests in populations at various degrees of adaptive potential, which we estimate on the basis of the remaining fraction of beneficial mutations in the DFE_β for the most common genotype. The invasion probability is estimated as the fraction of n_{reps} replicates in which a lineage from the original subpopulation becomes the most common genotype in the population. For an estimated invasion probability p, the precision of the estimate is given by the standard deviation of a binomial random variable: $(p(1-p)/n_{\mathrm{reps}})^{1/2}$.

Table 3: Simulation parameters and their default values

Parameter	Symbol	Default value
Genome length	N	100
Epistasis degree	K	0, 1, or 2
Mutation rate (per genome per generation)	μ	10^{-4}
Initial number of genotypes		50
Initial population size for genotype i	n_{i0}	100
Carrying capacity	κ	5,000

Parameter Values

Unless otherwise indicated, our simulations used a sequence of length $N = 100$ and epistasis parameter $K = 0$ (no epistasis) or $K = 1$ or 2. We used a carrying capacity of $\kappa = 5{,}000$ and initialized simulations with 50 random genotypes, each with $n_{i0} = 100$ individuals. We note that for a randomly generated genotype in the *NK* model, 50% of mutations are expected to be beneficial.

The default sequence mutation rate in the simulations was $\mu = 0.0001$ per genome per generation, the order of magnitude of *E. coli* K12 (Sane et al. 2023). Invasion success is determined after 5,000 generations. Note that our results were not sensitive to this final time as long as it was sufficiently large. See table 3 for a list of simulation parameters and default values.

Results

Adaptive Substitutions Reflect the Mutational Bias

Using differences between the most common genotype and its closest genetic relative in the founding population as a proxy for fixation, figure 2*a* demonstrates that the mutation bias is strongly reflected in the substitutions that occur as the population adapts. In the illustrated case, a bias of $\beta = 0.7$ (70% transition probability) results in the number of fixed transitions exceeding fixed transversions, even though there are twice as many available transversions as transitions.

In figure 2*b*, we plot the fraction of fixations that are transitions, versus time, for different values of the mutation bias. It is clear from the figure that substitutions reflect the bias strongly, particularly at early times. As adaptation proceeds, the overrepresented class fixes relatively less often as beneficial mutations of that class are depleted. If mutation is unbiased, $\beta = 1/3$, one-third of substitutions are transitions as expected, and this value remains constant. The standard error of means in the fraction of transition fixations is high for the first few thousand generations due to the low number of fixations (on average across all biases, less than 1 mutation fixes at generation 1,000, while only 5.5 mutations fix at 5,000 generations). Thus, results are shown starting at generation 10,000 in figure 2*b*.

The Fraction of Beneficial Mutations in the Oversampled Mutation Class Rapidly Declines

As beneficial mutations in oversampled mutation classes fix more frequently than those in undersampled classes, our analytical work predicts that this reduces the beneficial fraction of the DFE for oversampled classes. We first confirm this effect in full populations by simulating the evolution of either transition- or transversion-biased populations, recording the beneficial fraction of all possible transitions, f_{Ti}, and all possible transversions, f_{Tv}, for the most common genotype in the population at any time.

Figure 3 shows results for a transition-biased population with $\beta = 0.7$, consistent with a twofold excess of transitions above the null expectation (Stoltzfus and McCandlish 2017). Although the beneficial fraction is initially the same in both mutational classes, f_{Ti} decays more quickly than f_{Tv} (fig. 3*a*). The overall beneficial fraction declines but remains between f_{Ti} and f_{Tv}. As a result of their different decay rates, the difference between f_{Ti} and f_{Tv} increases with time as beneficial transitions fix more often than beneficial transversions and is significantly different from zero except at very early time points (fig. 3*b*). After 100,000 generations, there are roughly twice as many beneficial transversions as transitions available (fig. 3*b*); this factor of two also reflects the maximum possible increase in the beneficial fraction for a bias-shifted strain, equivalent to the factor G in the heuristic argument above, for an extreme bias shift from transitions to transversions. Although this factor could increase further at later times, the simulated populations have little remaining adaptive potential at the end of the simulation time.

In addition, transversions exceed transitions not only in their beneficial fraction but also in the mean magnitude of the positive selection coefficient; in other words, as evolution progresses a single beneficial transversion is expected to be more advantageous than a single beneficial transition (fig. 3*c*, 3*d*). At the end of the simulation time, the effect size of a beneficial transversion was about 1.5-fold higher than a beneficial transition, corresponding to factor H in the heuristic argument.

As evolution proceeds and the beneficial fraction of the DFE is reduced, the deleterious fraction concomitantly increases. Again, the deleterious fraction for both mutational classes is initially 50%, but the deleterious fraction for the oversampled class, d_{Ti}, increases more quickly than d_{Tv} (fig. 3*e*). The difference between d_{Ti} and d_{Tv} increases in magnitude over time (fig. 3*f*), but the effect is more modest than the changes observed in the beneficial fraction. After

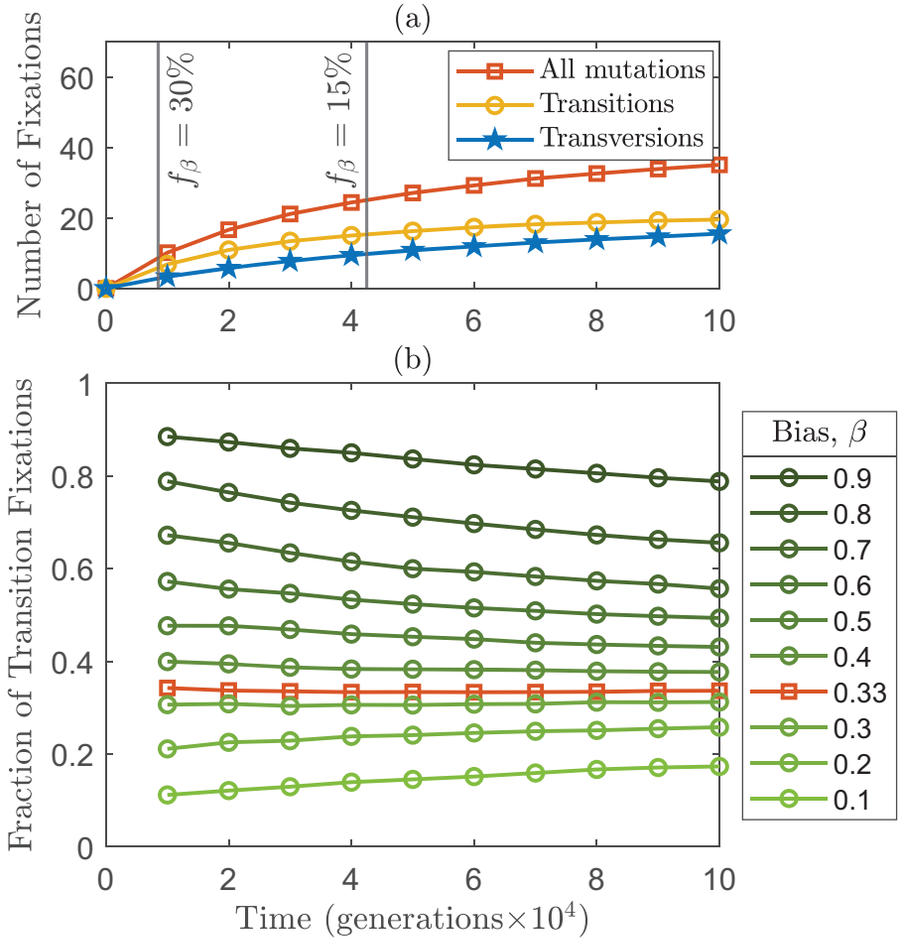

Figure 2: Mutational bias affects the numbers of transition/transversion fixations. *a*, More transitions (circles) than transversions (stars) fix in a transition-biased population ($\beta = 0.7$) with epistasis ($K = 1$). Hamming distance to the closest ancestor is shown by squares. The two vertical lines indicate when the beneficial fraction reaches 30% and 15%. *b*, The fraction of fixations that are transitions (means of 300 replicates) is almost constant for unbiased mutations (squares), while it strongly reflects the bias in other cases. As adaptation proceeds, this fraction decreases for transition-biased and increases for transversion-biased populations. Error bars are smaller than symbol heights and are omitted.

100,000 generations, the difference in the deleterious fraction is less than 5%. Overall, the observed increase in the deleterious fraction predicts a modest increase in the deleterious load for an oversampled mutational class. We note for completeness that the mean negative selection coefficient changes only negligibly during evolution (see fig. S2); differences between the deleterious selective effect for transitions and transversions were at most 2%. Filled circles in figure 3*b*, 3*d*, and 3*f* indicate that the difference $f_{\mathrm{Tv}} - f_{\mathrm{Ti}}$ is significantly different from zero at that time (*t*-test, $P < .05$).

The qualitative behaviors observed in figure 3 were robust across the parameter ranges we tested, including smooth fitness landscapes (fig. S3, $K = 0$) and for a lower degree of epistasis (fig. S4, $K = 1$). The magnitude of these effects is reduced for weaker transition biases (fig. S5, $\beta = 0.5$) and is reversed when the population is initially transversion biased (fig. S6, $\beta = 0.1$).

Bias Reversals Increase the Invasion Probability of Mutators and Can Reverse the Expected Outcome of Invasion

Given the potential increase in beneficial fraction afforded by a bias shift, we next asked whether strains with a bias shift would invade a wild-type population. Figure 4 shows results for both smooth (blue) and epistatic (red) fitness landscapes, for populations at two degrees of adaptive potential (30% [*left*] and 15% [*right*] remaining beneficial mutations), and for the limiting case of a full bias shift ($\beta = 1 \rightarrow \beta' = 0$; *top*) and a second case of a strong bias shift ($\beta = 0.9 \rightarrow \beta' = 0.1$; *bottom*).

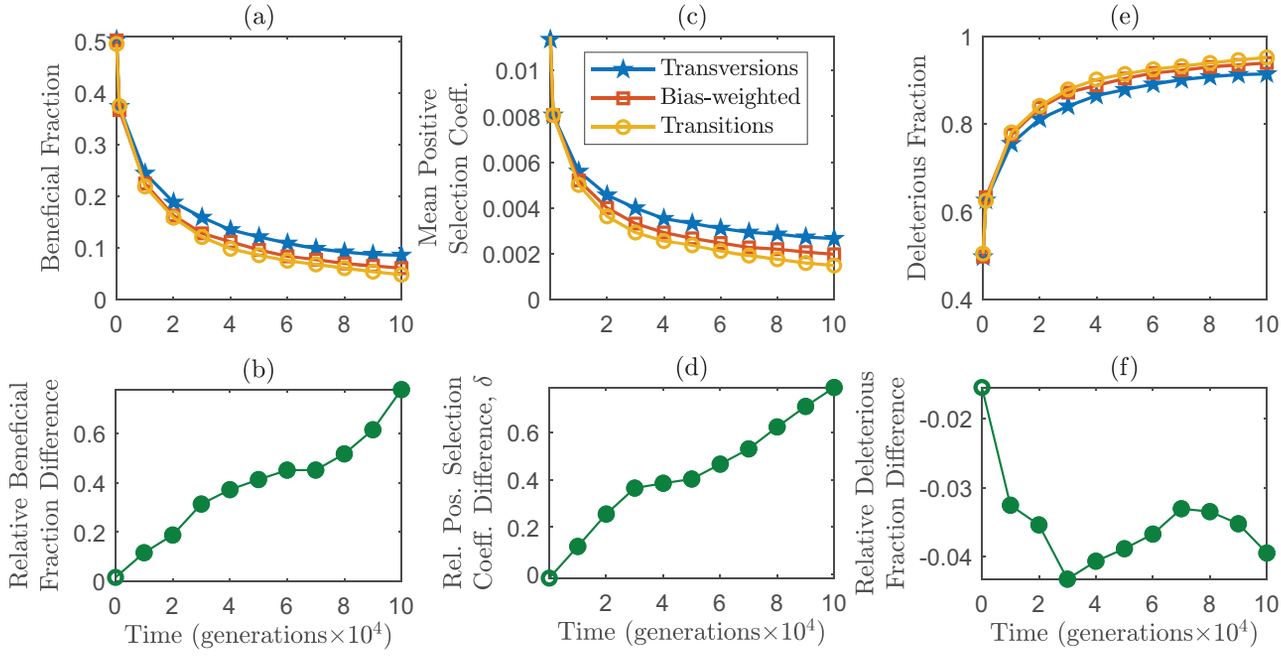

Figure 3: Beneficial fractions and beneficial effect sizes decline during the evolution of a transition-biased population, while deleterious fractions increase. *a*, The fraction of beneficial transitions (circles) decreases over time, falling more rapidly than beneficial transversions (stars). The overall beneficial fraction of the bias-weighted distribution of fitness effects of mutations (f_β, squares) falls in between. *b*, The relative difference $(f_{\text{Tv}} - f_{\text{Ti}})/f_{\text{Ti}}$ increases over time. *c* and *d* show analogous results for the mean positive effect sizes, while *e* and *f* show the opposite for the deleterious fractions. Means of 300 replicates are shown for $\beta = 0.7$ and $K = 2$. Error bars in top panels are smaller than symbol heights and are omitted.

As a comparison, we tested the invasion probability of mutator strains with an *F*-fold increase in mutation rate (*x*-axis) but no change in the mutation spectrum (solid lines). On the left edge of each panel (*y*-intercepts), we confirm that strains that change neither the mutation rate nor the bias have an invasion probability of 5%, which is the neutral expectation when seeded at an initial frequency of 5%. As the mutation rate multiple, *F*, is increased, mutator strains are initially favored (have an invasion probability higher than neutral), particularly in populations with more adaptive potential (*left*). Further increases in mutation rate become disfavored, however, as the deleterious load overwhelms the benefit of accessing beneficial mutations more easily. In general we see that mutators are strongly favored when many beneficial mutations are available (*left*), but high mutation rates are disadvantageous when the population is closer to the fitness peak (*right*). We also note that mutators are favored on epistatic landscapes (solid red vs. solid blue), presumably because of an enhanced ability to cross fitness valleys on rugged landscapes.

We then tested shifts in mutation bias (dashed lines). The left edge (*y*-intercept) of each panel thus shows the invasion probability for a strain that has a bias shift (dashed lines) but no change in mutation rate; in all cases, the bias shift increases the invasion probability above the neutral expectation, but even in the most extreme case ($f_\beta = 15\%$ and $\beta = 1 \rightarrow \beta' = 0$) the advantage of the bias-shifted strain is rather modest.

The effect of a bias shift can be dramatically increased, however, for mutator strains (dashed lines vs. solid lines at $F > 1$). In all cases, mutators have substantially higher invasion probabilities if they also reverse the mutation bias. As predicted theoretically, in all cases the bias shift extends the range of mutation rates over which mutators are favored. For mutator strains with very high mutation rates, the invasion probability can change from below the neutral expectation or near zero, without the bias shift, to values as high as 20%–40%. We also point out that the effect of combining an increase in mutation rate with a bias shift, in these full population simulations, is highly nonlinear. If we take as an example the smooth fitness landscape (blue lines) in figure 4*b*, a 100-fold increase in mutation rate alone reduces the invasion probability below the neutral expectation, while the bias shift alone increases the invasion probability by a factor of just over 2 (*y*-intercept). However, a strain that both shifts the bias and

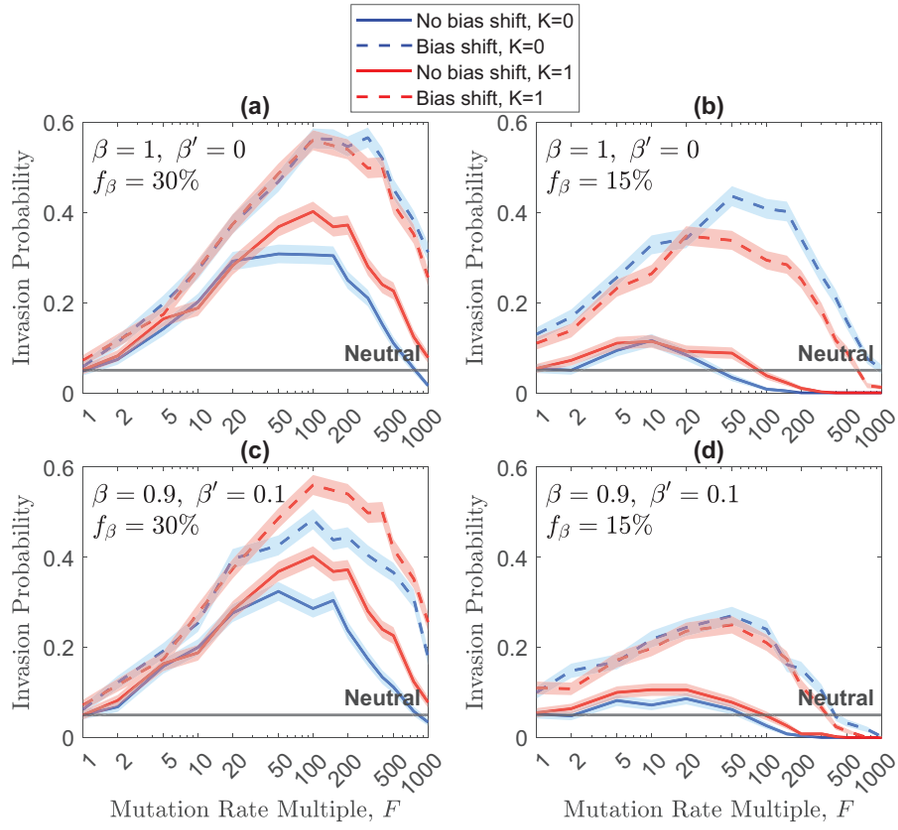

Figure 4: Bias-shifted mutators have higher invasion probabilities (dashed lines) than mutators without a bias shift (solid lines). Invading strains are initiated at 5% frequency and have F-fold increase in mutation rate; we compare no change in bias with full bias shift ($\beta = 1$ to $\beta' = 0.1$, *top*) or strong bias shift ($\beta = 0.9$ to $\beta' = 0.1$, *bottom*). Invasion tests occur at two levels of adaptive potential, $f_\beta = 30\%$ (*left*) and $f_\beta = 15\%$ (*right*). The case of epistasis is shown in red, while for blue lines $K = 0$. The horizontal lines represent the neutral expectation 0.05. Results from 500 replicates are shown; shaded regions indicate ±1 SD.

increases the mutation rate 100-fold has an invasion probability that is eightfold higher than neutral.

The Direction of the Bias Shift Relative to an Unbiased Spectrum Determines the Effect of the Shift

Having established that bias shifts, at least in these extreme cases ($1 \to 0$ and $0.9 \to 0.1$), are more likely to emerge when coupled with changes in mutation rate, we now investigate bias shifts at a range of directions and magnitudes on the fate of mutator strains.

As described in the "Theory" section, the effect of a bias shift depends on the unbiased mutation frequency, α; the bias with which the population has been evolving prior to the shift, β; and the shifted bias β'. Figure 5 shows how this applies to the transition-transversion ratio, where $\alpha = 1/3$. We first investigate changes in the preexisting bias, β. In particular, after populations have evolved with various values of β, we quantify the invasion probability of a mutator strain with a 50-fold increase in mutation rate, comparing the fate of this mutator strain without a bias shift (solid lines) to its fate with a bias shift (dashed lines). Results for two values of β' are shown in figure 5. Figure 5*a* shows that when the population is initially transition biased (to the right of the vertical line), a shift to $\beta' = 0.9$ reinforces the previous bias and the invasion probability is reduced by the bias shift; in contrast, if the population is initially transversion biased (to the left of the vertical line), a bias shift to $\beta' = 0.9$ reverses the existing bias and increases the invasion probability. These two effects are reversed when the bias shifts to $\beta' = 0.1$, as shown in figure 5*b*. Results for reinforcements in figure 5*b* are not significantly different with and without bias shifts, presumably because of the limited possible magnitude of bias shifts in this region. Results are shown for both smooth and epistatic fitness landscapes and for populations at an adaptive potential of 15% remaining beneficial mutations. Similar results are obtained when the mutators have

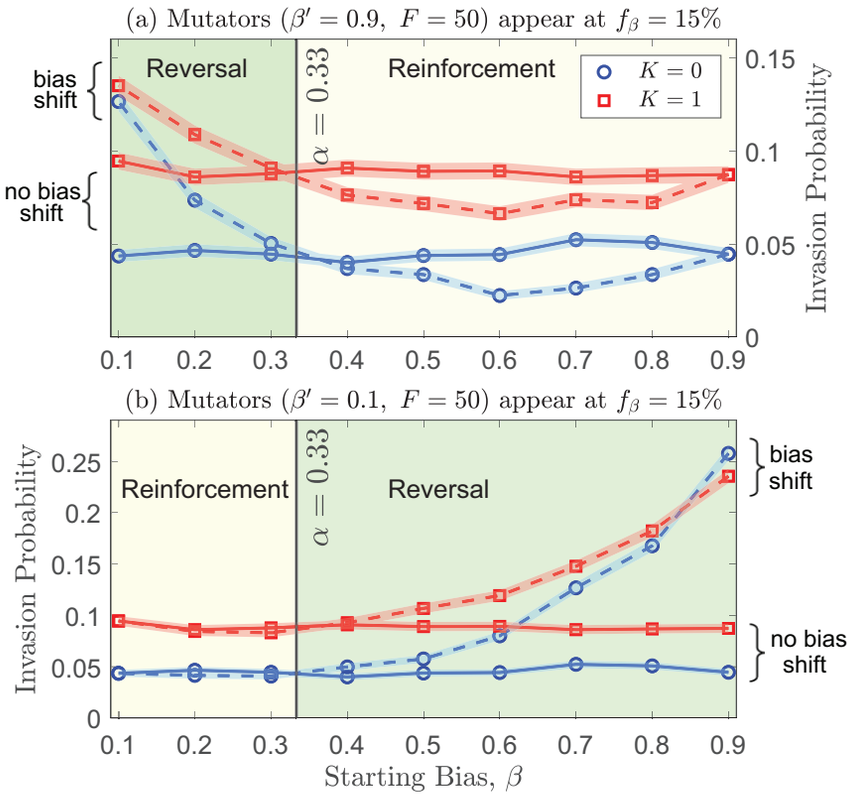

Figure 5: Mutator invasion probability increases when bias is reversed. Populations evolved with a starting bias β until 15% beneficial fraction was reached before invasion tests for mutators ($F = 50$) were initiated. Mutators either have the same bias (solid lines) or shifted bias (dashed lines). The vertical line represents the unbiased transition frequency. *a*, For $\beta < \alpha$, a shift to $\beta' = 0.9$ reverses the bias and thus increases the invasion probability; the same bias shift tends to reduce the probability if $\beta > \alpha$. *b*, The effects are reversed when the bias shifts to $\beta' = 0.1$. Results from 4,000 replicates are shown; shaded regions indicate ±1 SD.

a 10-fold-higher mutation rate (fig. S7) as well as at an earlier time when the beneficial fraction is 30%, either for the same mutation rate multiple of $F = 50$ (fig. S8) or for $F = 200$ (fig. S9). The advantage of a bias reversal is more striking when $f_\beta = 15\%$; at this stage the DFE for the ancestor is depleted and the bias shift becomes a key factor in the competition between ancestor and mutator.

Stronger Bias Reversals Increase the Invasion Probability

While the direction of the bias shift establishes whether it is beneficial, the magnitude of the shift determines the magnitude of the benefit. Figure 6 shows that stronger reversals have a higher invasion probability, again in the presence or absence of epistasis and for populations relatively early and later in adaptation. In contrast with figure 5, here we fix the starting bias, $\beta = 0.9$, and shift the bias to various values of β'. Thus, bias reversals occur when the new bias β' is smaller than the unbiased value $\alpha = 1/3$; in this case the spectrum changes from transition to transversion biased. Bias reductions occur when $\beta' < \beta$ but $\beta' > \alpha$; the new spectrum is still transition biased but is less extreme. When $\beta' > 0.9$, the bias is reinforced. We note that the influence of the bias shift is greater (steeper slope in fig. 6*a*) at $f_\beta = 15\%$ than at $f_\beta = 30\%$, again presumably because the bias shift is less critical to "finding" a beneficial mutation when there are more beneficial mutations available. Invasions are tested for mutator strains with a 50-fold increase in the mutation rate in figure 6*a*, whereas in figure 6*b* tests are performed for mutation rate multiples $F = 10$, 50, and 200. All of these simulations give the same qualitative results, illustrating the advantage of reducing or reversing a prevailing bias.

Discussion

Multiple factors can affect the evolution of the mutation rate and spectrum. Population genetics theory predicts that for a given number of functional sites in the genome,

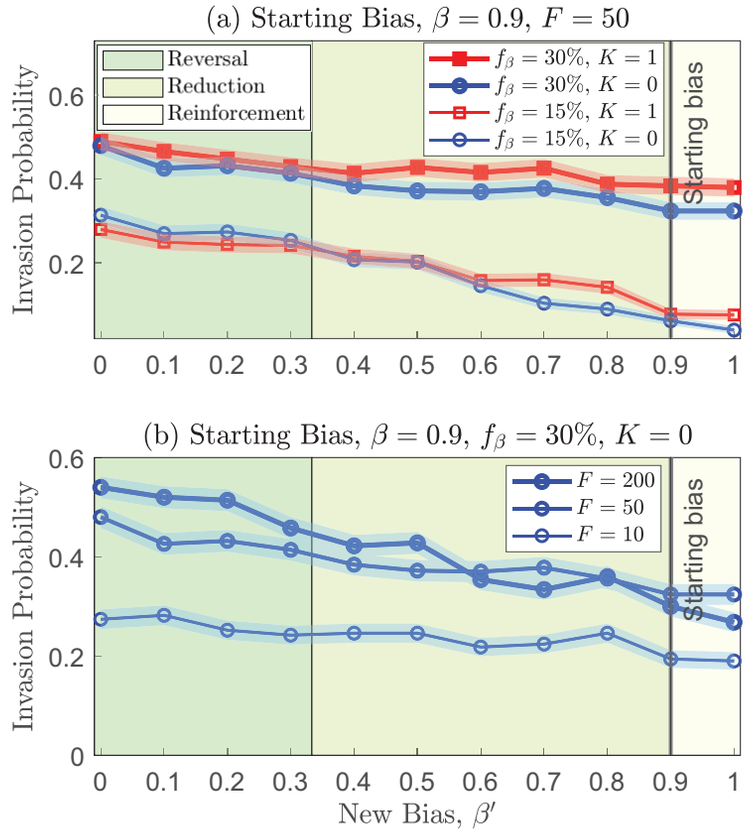

Figure 6: In populations that have evolved with a transition frequency of $\beta = 0.9$, the invasion probability of mutators increases when the bias is reduced or reversed. *a*, Larger bias reversals increased the invasion probability of mutators with 50-fold higher mutation rate whether the invasion test occurred at a beneficial fraction of 30% (bold lines) or 15% (thin lines), on either smooth ($K = 0$, blue circles) or epistasic ($K = 1$, red squares) landscapes. *b*, Results are consistent across different values of the mutation rate multiplier, F ($K = 0, f_\beta = 30\%$ illustrated.) Results from 500 replicates are shown; shaded regions indicate ±1 SD.

the larger the effective population size, the greater the power of natural selection to reduce the mutation rate (drift-barrier hypothesis; Lynch 2011; Sung et al. 2012). In animals, selection on most sequence-dependent DNA repair enzymes, which could alter the mutation spectrum within a genome, is likely to fall below the threshold at which natural selection is effective (Harris and Pritchard 2017). However, there is the possibility that in natural populations DNA sequence-dependent hypo-/hypermutators could segregate if the burden of new mutations is big enough. For example, a natural hypomutator allele reducing the mutation rate of C → A mutations has been recently discovered in mice (Sasani et al. 2022). In humans, the TCC → TTC mutation rate increased in Europeans 15,000 to 2,000 years ago (Harris and Pritchard 2017), but it is unknown whether this was driven by an environmental mutagen or a hypermutator allele that temporarily rose in frequency. In fungi, it has been recently described how the presence/absence of 52 DNA mismatch repair (MMR) genes impacts the mutation spectrum across more than 1,000 species, finding that in pathogenic species the loss of MMR genes is substantial and has probably increased their mutation rate (Phillips et al. 2021). In human tumors, mutations on MMR genes have a characteristic signature in the mutation spectrum (Alexandrov et al. 2013) that can be recovered in *Caenorhabditis elegans* when mutating the same genes (Meier et al. 2018). Other DNA repair pathways and genomic integrity checkpoints, such as Rad53p (human homolog Chk2), have been described to be downregulated in fungal pathogens (Shor et al. 2020; Steenwyk 2021). These empirical works highlight the complex interaction between population size and the environment as drivers of mutation rate and spectrum evolution, as well as possibly also mutation bias evolution. Finally, apart from the number of functional sites in the genome, other genomic attributes, such as the recombination rate, can also impact the efficacy of natural selection on mutation rate modifiers (sequence context dependent or not). Increasing

the recombination rate is expected to reduce the efficacy of selection because an allele that increases/decreases the mutation rate can recombine away from deleterious mutations it generates elsewhere in the genome (Lynch 2011).

Despite these multiple interacting factors, previous work has also provided compelling evidence that changing the mutation spectrum alone can drive both the emergence and decay of mutators (Couce et al. 2013, 2017; Couce and Tenaillon 2019). Here, we provide a mechanistic and general explanation of why, and under what conditions, these effects might occur. In particular, we demonstrate that when a spectrum change either reduces or reverses an existing bias—that is, a bias that has persisted over a period of adaptation—that spectrum change will both increase the beneficial fraction of the DFE and increase the mean selective effect of beneficial mutations.

Our analytical approach, while necessarily simplified, demonstrates mathematically that after a period of adaptation, bias reductions or reversals are expected to increase the beneficial fraction of the DFE and that this effect will be stronger with larger magnitude reversals. This prediction is confirmed in simulations that relax several simplifying assumptions, treating full populations under both clonal interference and epistasis.

Despite these robust changes to the DFE when the mutation bias is reduced or reversed, a surprising result of our study is that in the absence of changes to mutation rate, the invasion probability of bias-shifted strains is only modestly increased, even under very strong bias reversals (fig. 4, *y*-intercepts). This is because both increases in the beneficial fraction of the DFE and increases in the positive selective effect are of the order of several fold, while mutation rate increases may be 50–100-fold or more (Denamur and Matic 2006). For example, a bias shift that doubles the beneficial fraction ($G = 2$) and increases the positive selective effect by 50% ($H = 1.5$) alters the DFE substantially (fig. 3) but would confer only a threefold advantage ($GH = 3$) over the wild type in generating beneficial fixations.

In contrast, as observed for mutations with increased beneficial effect (Couce et al. 2013), bias shifts can dramatically alter the fate of mutator strains (fig. 4). When a shift in the bias is coupled with an increase in mutation rate, the invasion probability of the strain can be vastly increased, including cases in which a disfavored increase in the mutation rate becomes strongly favored if coupled with a bias reduction or reversal. This is due to three effects: (1) the expected value of the selection coefficient for beneficial mutations is increased by the bias shift, (2) the fraction of mutations that are beneficial is increased, and (3) as the beneficial fraction is increased, the fraction of mutations that are deleterious is concomitantly reduced. Of these three effects, in our simulated landscapes the increase in beneficial fraction had the greatest magnitude, while the reduction in deleterious load was modest. Further work on empirical fitness landscapes that quantify the DFE for bias-shifted strains (Couce et al. 2013; Sane et al. 2023) is necessary to determine which effects might dominate in natural settings.

We also note that after a change in mutation rate, load accrues gradually; thus, mutator strains in our invasion tests may invade before the equilibrium load is realized. This extends the range of mutation rates over which the mutator strain invades beyond the theoretical prediction, which assumed equilibrium load. Since load would also accrue gradually in natural settings after a loss of DNA repair function, our theoretical prediction is conservative, underestimating the success of bias-shifted mutators. More accurate predictions could include the dynamics of mutational load after a sudden change in mutation rate.

The effects we describe are relevant to asexual evolution, in which changes to mutation rate and/or bias remain linked to the beneficial mutations they generate for sufficient time to reach fixation. Previous work suggests that for mutation rate modifiers, modest levels of horizontal gene transfer or recombination substantially reduce the mutator advantage (Johnson 1999; Tenaillon et al. 2000). We note that DNA repair enzymes in bacteria are frequently gained and lost, resulting in well-studied changes in mutation rate (Denamur and Matic 2006; Sane et al. 2023). Changes in mutation spectrum with these gains and losses can also be extreme: a Ti fraction of less than 5% is obtained with the knockout of the enzyme mutT (Foster et al. 2015), while a Ti fraction of greater than 95% occurs with the loss of mutL (Lee et al. 2012). Invasion simulations that test bias shifts and mutation rates estimated in specific bacterial knockout strains are thus another clear avenue for future work.

Acknowledgments

This work was supported by the Natural Sciences and Engineering Research Council of Canada (grant RGPIN-2019-06294) and by the National Institute of General Medical Sciences of the National Institutes of Health (grant R01GM127348). We thank Deepa Agashe and Mrudula Sane for helpful discussions and the reviewers for insightful comments that strengthened the work.

Statement of Authorship

M.Z.T., D.C., R.N.G., and L.M.W. designed the study. L.M.W., M.Z.T., and S.V. wrote the simulation code. M.Z.T. and S.V. generated simulation data. M.Z.T., D.C., R.N.G., and L.M.W. analyzed and interpreted simulation data.

M.Z.T. and L.M.W. derived the theory and drafted the manuscript. All authors edited and finalized the manuscript.

Data and Code Availability

Code and data can be accessed via the Dryad Digital Repository (https://doi.org/10.5061/dryad.qz612jmk2; Tuffaha et al. 2023).

Literature Cited

Alexandrov, L. B., S. Nik-Zainal, D. C. Wedge, S. A. Aparicio, S. Behjati, A. V. Biankin, G. R. Bignell, et al. 2013. Signatures of mutational processes in human cancer. Nature 500:415–421.

Cano, A. V., and J. L. Payne. 2020. Mutation bias interacts with composition bias to influence adaptive evolution. PLoS Computational Biology 16:e1008296.

Cano, A. V., H. Rozhonová, A. Stoltzfus, D. M. McCandlish, and J. L. Payne. 2022. Mutation bias shapes the spectrum of adaptive substitutions. Proceedings of the National Academy of Sciences of the USA 119:e2119720119.

Couce, A., N. Alonso-Rodriguez, C. Costas, A. Oliver, and J. Blázquez. 2016. Intrapopulation variability in mutator prevalence among urinary tract infection isolates of *Escherichia coli*. Clinical Microbiology and Infection 22:566.e1–566.e7.

Couce, A., L. V. Caudwell, C. Feinauer, T. Hindré, J.-P. Feugeas, M. Weigt, R. E. Lenski, D. Schneider, and O. Tenaillon. 2017. Mutator genomes decay, despite sustained fitness gains, in a long-term experiment with bacteria. Proceedings of the National Academy of Sciences of the USA 259:E9026–E9035.

Couce, A., J. R. Guelfo, and J. Blázquez. 2013. Mutational spectrum drives the rise of mutator bacteria. PLoS Genetics 9:e1003167.

Couce, A., and O. Tenaillon. 2019. Mutation bias and GC content shape antimutator invasions. Nature Communications 10:3114.

Denamur, E., and I. Matic. 2006. Evolution of mutation rates in bacteria. Molecular Microbiology 60:820–827.

Ewens, W. J. 2012. Mathematical population genetics. I. Theoretical introduction. 2nd ed. Vol. 27. Interdisciplinary Applied Mathematics. Springer, New York.

Foster, P. L., H. Lee, E. Popodi, J. P. Townes, and H. Tang. 2015. Determinants of spontaneous mutation in the bacterium *Escherichia coli* as revealed by whole-genome sequencing. Proceedings of the National Academy of Sciences of the USA 112:E5990–E5999.

Fox, E. J., M. J. Prindle, and L. A. Loeb. 2013. Do mutator mutations fuel tumorigenesis? Cancer and Metastasis Reviews 32:353–361.

Giraud, A., I. Matic, O. Tenaillon, A. Clara, M. Radman, M. Fons, and F. Taddei. 2001. Costs and benefits of high mutation rates: adaptive evolution of bacteria in the mouse gut. Science 291:2606–2608.

Gitschlag, B. L., A. V. Cano, J. L. Payne, D. M. McCandlish, and A. Stoltzfus. 2023. Mutation and selection induce correlations between selection coefficients and mutation rates. American Naturalist 202:534–557.

Gomez, K., J. Bertram, and J. Masel. 2020. Mutation bias can shape adaptation in large asexual populations experiencing clonal interference. Proceedings of the Royal Society B 287:20201503.

Harris, K., and J. K. Pritchard. 2017. Rapid evolution of the human mutation spectrum. eLife 6:e24284.

Hodgkinson, A., and A. Eyre-Walker. 2011. Variation in the mutation rate across mammalian genomes. Nature Reviews Genetics 12:756–766.

Jiang, P., A. R. Ollodart, V. Sudhesh, A. J. Herr, M. J. Dunham, and K. Harris. 2021. A modified fluctuation assay reveals a natural mutator phenotype that drives mutation spectrum variation within *Saccharomyces cerevisiae*. eLife 10:e68285.

Johnson, T. 1999. Beneficial mutations, hitchhiking and the evolution of mutation rates in sexual populations. Genetics 151:1621–1631.

Katju, V., and U. Bergthorsson. 2019. Old trade, new tricks: insights into the spontaneous mutation process from the partnering of classical mutation accumulation experiments with high-throughput genomic approaches. Genome Biology and Evolution 11:136–165.

Kessler, D. A., and H. Levine. 1998. Mutator dynamics on a smooth evolutionary landscape. Physical Review Letters 80:2012–2015.

LeClerc, J. E., B. Li, W. L. Payne, and T. A. Cebula. 1996. High mutation frequencies among *Escherichia coli* and *Salmonella* pathogens. Science 274:1208–1211.

Lee, H., E. Popodi, H. Tang, and P. L. Foster. 2012. Rate and molecular spectrum of spontaneous mutations in the bacterium *Escherichia coli* as determined by whole-genome sequencing. Proceedings of the National Academy of Sciences of the USA 109:E2774–E2783.

Leigh, E. G. 1970. Natural selection and mutability. American Naturalist 104:301–305.

Lenski, R. E. 2004. Phenotypic and genomic evolution during a 20,000-generation experiment with the bacterium *Escherichia coli*. Plant Breeding Reviews 24:225–265.

Lynch, M. 2011. The lower bound to the evolution of mutation rates. Genome Biology and Evolution 3:1107–1118.

Lynch, M., M. S. Ackerman, J.-F. Gout, H. Long, W. Sung, W. K. Thomas, and P. L. Foster. 2016. Genetic drift, selection and the evolution of the mutation rate. Nature Reviews Genetics 17:704–714.

Macken, C. A., and A. S. Perelson. 1989. Protein evolution on rugged landscapes. Proceedings of the National Academy of Sciences of the USA 86:6191–6195.

MacLean, R. C., A. R. Hall, G. G. Perron, and A. Buckling. 2010. The population genetics of antibiotic resistance: integrating molecular mechanisms and treatment contexts. Nature Reviews Genetics 11:405–414.

Maharjan, R. P., and T. Ferenci. 2017. A shifting mutational landscape in 6 nutritional states: stress-induced mutagenesis as a series of distinct stress input–mutation output relationships. PLoS Biology 15:e2001477.

Martincorena, I., and N. M. Luscombe. 2013. Non-random mutation: the evolution of targeted hypermutation and hypomutation. BioEssays 35:123–130.

Matic, I., M. Radman, C. Taddei, F. B. Picard, C. Doit, E. Bingen, E. Denamur, and J. Elion. 1997. Highly variable mutation rates in commensal and pathogenic *Escherichia coli*. Science 277:1833–1834.

Maynard Smith, J., and J. Haigh. 1974. The hitch-hiking effect of a favourable gene. Genetics Research 23:23–35.

Meier, B., N. V. Volkova, Y. Hong, P. Schofield, P. J. Campbell, M. Gerstung, and A. Gartner. 2018. Mutational signatures of DNA

mismatch repair deficiency in *C. elegans* and human cancers. Genome Research 28:666–675.
Miyake, T. 1960. Mutator factor in *Salmonella typhimurium*. Genetics 45:11–14.
Monroe, J. G., T. Srikant, P. Carbonell-Bejerano, C. Becker, M. Lensink, M. Exposito-Alonso, M. Klein, et al. 2022. Mutation bias reflects natural selection in *Arabidopsis thaliana*. Nature 602:101–105.
Oliver, A., R. Cantón, P. Campo, F. Baquero, and J. Blàzquez. 2000. High frequency of hypermutable *Pseudomonas aeruginosa* in cystic fibrosis lung infection. Science 288:1251–1253.
Payne, J. L., F. Menardo, A. Trauner, S. Borrell, S. M. Gygli, C. Loiseau, S. Gagneux, and A. R. Hall. 2019. Transition bias influences the evolution of antibiotic resistance in *Mycobacterium tuberculosis*. PLoS Biology 17:e3000265.
Phillips, M. A., J. L. Steenwyk, X.-X. Shen, and A. Rokas. 2021. Examination of gene loss in the DNA mismatch repair pathway and its mutational consequences in a fungal phylum. Genome Biology and Evolution 13:evab219.
Raghavan, V., C. F. Aquadro, and E. Alani. 2019. Baker's yeast clinical isolates provide a model for how pathogenic yeasts adapt to stress. Trends in Genetics 35:804–817.
Richardson, A. R., Z. Yu, T. Popovic, and I. Stojiljkovic. 2002. Mutator clones of *Neisseria meningitidis* in epidemic serogroup A disease. Proceedings of the National Academy of Sciences of the USA 99:6103–6107.
Ridderberg, W., K. J. Handberg, and N. Nørskov-Lauritsen. 2020. Prevalence of hypermutator isolates of *Achromobacter* spp. from cystic fibrosis patients. International Journal of Medical Microbiology 310:151393.
Sane, M., G. D. Diwan, B. A. Bhat, L. M. Wahl, and D. Agashe. 2023. Shifts in mutation spectra enhance access to beneficial mutations. Proceedings of the National Academy of Sciences of the USA 120:e2207355120.
Sasani, T. A., D. G. Ashbrook, A. C. Beichman, L. Lu, A. A. Palmer, R. W. Williams, J. K. Pritchard, and K. Harris. 2022. A natural mutator allele shapes mutation spectrum variation in mice. Nature 605:497–502.
Shaver, A. C., P. G. Dombrowski, J. Y. Sweeney, T. Treis, R. M. Zappala, and P. D. Sniegowski. 2002. Fitness evolution and the rise of mutator alleles in experimental *Escherichia coli* populations. Genetics 162:557–566.
Shewaramani, S., T. J. Finn, S. C. Leahy, R. Kassen, P. B. Rainey, and C. D. Moon. 2017. Anaerobically grown *Escherichia coli* has an enhanced mutation rate and distinct mutational spectra. PLoS Genetics 13:e1006570.
Shor, E., R. Garcia-Rubio, L. DeGregorio, and D. S. Perlin. 2020. A noncanonical DNA damage checkpoint response in a major fungal pathogen. mBio 11:e03044-20.
Sniegowski, P. D., P. J. Gerrish, and R. E. Lenski. 1997. Evolution of high mutation rates in experimental populations of *E. coli*. Nature 387:703–705.
Soares, A. d. A., L. Wardil, L. B. Klaczko, and R. Dickman. 2021. Hidden role of mutations in the evolutionary process. Physical Review E 104:044413.
Steenwyk, J. L. 2021. Evolutionary divergence in DNA damage responses among fungi. mBio 12:e03348-20.
Stoltzfus, A. 2006. Mutation-biased adaptation in a protein NK model. Molecular Biology and Evolution 23:1852–1862.
Stoltzfus, A., and D. M. McCandlish. 2017. Mutational biases influence parallel adaptation. Molecular Biology and Evolution 34:2163–2172.
Stoltzfus, A., and R. W. Norris. 2015. On the causes of evolutionary transition : transversion bias. Molecular Biology and Evolution 33:595–602.
Stoltzfus, A., and L. Y. Yampolsky. 2009. Climbing mount probable: mutation as a cause of nonrandomness in evolution. Journal of Heredity 100:637–647.
Storz, J. F., C. Natarajan, A. V. Signore, C. C. Witt, D. M. McCandlish, and A. Stoltzfus. 2019. The role of mutation bias in adaptive molecular evolution: insights from convergent changes in protein function. Philosophical Transactions of the Royal Society B 374:20180238.
Sung, W., M. S. Ackerman, S. F. Miller, T. G. Doak, and M. Lynch. 2012. Drift-barrier hypothesis and mutation-rate evolution. Proceedings of the National Academy of Sciences of the USA 109:18488–18492.
Taddei, F., M. Radman, J. Maynard Smith, B. Toupance, P. H. Gouyon, and B. Godelle. 1997. Role of mutator alleles in adaptive evolution. Nature 387:700–702.
Tanaka, M. M., C. T. Bergstrom, and B. R. Levin. 2003. The evolution of mutator genes in bacterial populations: the roles of environmental change and timing. Genetics 164:843–854.
Tenaillon, O., H. L. Nagard, B. Godelle, and F. Taddei. 2000. Mutators and sex in bacteria: conflict between adaptive strategies. Proceedings of the National Academy of Sciences of the USA 97:10465–10470.
Tenaillon, O., B. Toupance, H. L. Nagard, F. Taddei, and B. Godelle. 1999. Mutators, population size, adaptive landscape and the adaptation of asexual populations of bacteria. Genetics 152:485–493.
Travis, J., and E. Travis. 2002. Mutator dynamics in fluctuating environments. Proceedings of the Royal Society B 269:591–597.
Treffers, H. P., V. Spinelli, and N. O. Belser. 1954. A factor (or mutator gene) influencing mutation rates in *Escherichia coli*. Proceedings of the National Academy of Sciences of the USA 40:1064–1071.
Tuffaha, M. Z., S. Varakunan, D. Castellano, R. N. Gutenkunst, and L. M. Wahl. 2023. Data from: Shifts in mutation bias promote mutators by altering the distribution of fitness effects. American Naturalist, Dryad Digital Repository, https://doi.org/10.5061/dryad.qz612jmk2.
Wei, W., W.-C. Ho, M. G. Behringer, S. F. Miller, G. Bcharah, and M. Lynch. 2022. Rapid evolution of mutation rate and spectrum in response to environmental and population-genetic challenges. Nature Communications 13:4752.
Wielgoss, S., J. E. Barrick, O. Tenaillon, M. J. Wiser, W. J. Dittmar, S. Cruveiller, B. Chane-Woon-Ming, C. Médigue, R. E. Lenski, and D. Schneider. 2012. Mutation rate dynamics in a bacterial population reflect tension between adaptation and genetic load. Proceedings of the National Academy of Sciences of the USA 110:222–227.
Wylie, C. S., C.-M. Ghim, D. Kessler, and H. Levine. 2009. The fixation probability of rare mutators in finite asexual populations. Genetics 181:1595–1612.